The FASEB Journal article fj.09-142646. Published online May 19, 2010.

Fluidizing effects of C-reactive protein on lung surfactant membranes: protective role of surfactant protein A

Alejandra Sáenz,* Almudena López-Sánchez,* Jonás Mojica-Lázaro,* Leticia Martínez-Caro,† Nicolas Nin,† Luís A. Bagatolli,‡ and Cristina Casals*,[1]

*Departamento de Bioquímica y Biología Molecular and Centro de Investigación Biomédica en Red (CIBER) Enfermedades Respiratorias, Facultad de Biología, Universidad Complutense de Madrid, Madrid, Spain; †Servicio de Cuidados Intensivos and CIBER de Enfermedades Respiratorias, Hospital Universitario de Getafe, Madrid, Spain; and ‡Department of Biochemistry and Molecular Biology, MEMPHYS-Center for Biomembrane Physics, University of Southern Denmark, Odense, Denmark

ABSTRACT **The purpose of this study was to investigate how surfactant membranes can be perturbed by C-reactive protein (CRP) and whether surfactant protein A (SP-A) might overcome CRP-induced surfactant membrane alterations. The effect of CRP on surfactant surface adsorption was evaluated *in vivo* after intratracheal instillation of CRP into rat lungs. Insertion of CRP into surfactant membranes was investigated through monolayer techniques. The effect of CRP on membrane structure was studied through differential scanning calorimetry and fluorescence spectroscopy and microscopy using large and giant unilamellar vesicles. Our results indicate that CRP inserts into surfactant membranes and drastically increases membrane fluidity, resulting in surfactant inactivation. At 10% CRP/phospholipid weight ratio, CRP causes disappearance of liquid-ordered/liquid-disordered phase coexistence distinctive of surfactant membranes. SP-A, the most abundant surfactant lipoprotein structurally similar to C1q, binds to CRP (K_d=56±8 nM), as determined by solid-phase binding assays and dynamic light scattering. This novel SP-A/CRP interaction reduces CRP insertion and blocks CRP effects on surfactant membranes. In addition, intratracheal coinstillation of SP-A+CRP into rat lungs prevents surfactant inhibition induced by CRP, indicating that SP-A/CRP interactions might be an important factor *in vivo* in controlling harmful CRP effects in the alveolus.—Sáenz, A., López-Sánchez, A., Mojica-Lázaro, J., Martínez-Caro, L., Nin, N., Bagatolli, L. A., Casals, C. Fluidizing effects of C-reactive protein on lung surfactant membranes: protective role of surfactant protein A. *FASEB J.* 24, 000–000 (2010). www.fasebj.org**

Key Words: membrane fluidity · lipid domains · fluorescence · lipid-protein interaction · protein-protein interaction · lung injury

CRP IS CONSIDERED THE prototypical acute-phase protein in humans and other animal species. After sepsis, acute myocardial infarction, or tissue damage, serum levels of CRP can increase as much as 1000-fold within 24 to 48 h, and the magnitude of this increase correlates with the extent of tissue injury or the severity of inflammation (1–4). CRP is structurally characterized by 5 identical, noncovalently associated, globular subunits arranged symmetrically around a central pore (1, 4). Each subunit is folded into two antiparallel β-sheets with a flattened jellyroll topology, and binds two Ca^{2+} ions with a K_d of 30 μM (5). Ca^{2+} ions participate in the binding of some of its ligands and stabilize the subunit structure and the pentamer integrity.

The principal ligand of CRP is phosphocholine, which is widely distributed in teichoic acids, capsular carbohydrates, and lipopolysaccharides of bacteria, fungi, and other microorganisms (1–4). CRP binds to normal cells, including platelets, phagocytes, and endothelial cells, and avidly binds to dead or damaged cells, in which membrane structure is altered and nuclear constituents, which are also ligands of CRP, are exposed (1–4). Once CRP is bound to pathogens or necrotic cells, the protein is recognized by C1q and efficiently activates the classical pathway of human complement (1–4) or can also elicit responses from phagocytic cells through binding to FcγR receptors (1–4, 6). Thus CRP could serve to recognize a wide range of pathogens and altered self-molecules, and mediate their elimination by acting as a component of the humoral arm of innate immunity. However, the available data indicate that CRP has potentially harmful, as well as protective effects. CRP seems to be directly involved in the pathogenesis of arteriosclerotic lesions (7) and to enhance tissue damage in acute myocardial infarction and other inflammatory diseases (4).

With respect to the lung, CRP is considered a systemic biomarker of reduced lung function (8) and a prognostic marker in chronic obstructive pulmonary

[1] Correspondence: Departamento de Bioquímica y Biología Molecular I, Facultad de Biología, Universidad Complutense de Madrid, 28040-Madrid. E-mail: ccasalsc@bio.ucm.es

doi: 10.1096/fj.09-142646

disease (9) and cystic fibrosis (10). Moreover, patients with acute lung injury (ALI) and ischemia-reperfusion injury after lung transplantation have elevated levels of CRP in both plasma and the bronchoalveolar lavage (BAL) (11, 12). BAL CRP could issue from alveolar cells stimulated by proinflammatory mediators (13–15) and/or from the blood. The influx of serum CRP into the alveolar fluid may occur as a consequence of impaired alveolar-capillary barrier. We found that CRP present in the cell-free BAL of transplanted lungs is recovered in the floating pulmonary surfactant fraction (16). This indicates that CRP binds to lung surfactant, which consists of a complicated network of extracellular membranes that overlies the alveolar epithelium (17). Surfactant counteracts the alveolar tendency to collapse during expiration by reducing surface tension to low values (17). In addition, pulmonary surfactant components are involved in host-defense (18). Several *in vitro* studies have shown that CRP impairs lung surfactant function (11, 16, 19–21). Interestingly, SP-A, pulmonary surfactant's most abundant lipoprotein by mass, is able to counteract the inhibitory effects of a number of serum proteins, including CRP (17, 21).

The main objectives of our study were to investigate: *1*) how surfactant membranes can be perturbed by CRP; *2*) the mechanisms by which SP-A might overcome CRP-induced surfactant membrane alterations; and *3*) whether intratracheal instillation of CRP in rat lungs damages surfactant activity *in vivo* and whether SP-A/CRP interactions are an important factor *in vivo*.

MATERIALS AND METHODS

Materials

Synthetic lipids, 1,2-dipalmitoyl-phosphatidylcholine (DPPC), 1-palmitoyl-2-oleoyl-phosphatidylglycerol (POPG), and palmitic acid (PA) were purchased from Avanti Polar Lipids (Birmingham, AL, USA). The organic solvents (methanol and chloroform) used to dissolve lipids were HPLC grade (Scharlau, Barcelona, Spain). The fluorescent probes 1,1′-dioctadecyl-3,3,3′, 3′-tetramethylindocarbocyanine perchlorate (DiI_{C18}), 6-lauroyl-2-(*N,N*-dimethylmino) naphthalene (LAURDAN), and 1,6-diphenyl-1,3,5-hexatriene (DPH), the FluoReporter Mini-Biotin-XX Protein Labeling Kit, and the free radical 2,2,6,6-tetramethyl-1-piperidinyloxy (TEMPO) were purchased from Molecular Probes (Eugene, OR, USA). All other reagents were of analytical grade and obtained from Merck (Darmstadt, Germany).

Proteins

Surfactant protein A was isolated from BAL of patients with alveolar proteinosis using a sequential butanol and octylglucoside extraction. The purity of SP-A was checked by 1-dimensional SDS-PAGE in 12% acrylamide under reducing conditions and mass spectrometry. The oligomerization state of SP-A was assessed by electrophoresis under nondenaturing conditions, electron microscopy, and analytical ultracentrifugation as reported elsewhere (22, 23). SP-A consisted of supratrimeric oligomers of at least 18 subunits. Each subunit had an apparent molecular weight of 36 kDa. Biotinylated SP-A was prepared as described previously for the labeling of SP-A with fluorescent Texas-Red (24). The structure and functional activity of biotinylated SP-A were similar to that of unlabeled SP-A. Human CRP was obtained from Sigma-Aldrich (St. Louis, MO). CRP was always stored in 20 mM Tris-HCl, pH 7.8, containing 150 mM NaCl and 2.5 mM Ca_2Cl to prevent spontaneous dissociation (1). The purity and structural characteristics of human CRP were checked by MALDI-TOF/TOF mass spectrometry, SDS-PAGE in 12% acrylamide, fluorescence spectroscopy, and dynamic light scattering. Pentameric CRP has an apparent molecular weight of 118 kDa.

In vivo administration of CRP and CRP+SP-A in rat lungs

Intratracheal instillation of human CRP with or without SP-A was performed in male Sprague-Dawley rats (Harlan Iberica, Barcelona, Spain) weighing 350–400 g. Animals were anesthetized with intraperitoneal ketamine (90 mg/kg) and diazepam (5 mg/kg). For mechanical ventilation, low volume tidal (V_T) ventilation (V_T=9 ml/kg) and positive end-expiratory pressure (PEEP) of 5 cmH_2O were used. The respiratory rate was 70 bpm, inspiratory time 0.3 s, expiratory time 0.56 s, and FiO_2 0.35. All animals received humane care in accordance with the *Guide for the Care and Use of Laboratory Animals* (25).

Animals were divided randomly into 3 groups: control group (n=5); CRP-instilled group (n=5); and CRP/SP-A-coinstilled group (n=5). All animals were ventilated for an equilibration period of 30 min using the low V_T ventilation parameters described above. Then, human CRP was instilled at 37°C under sterile conditions at different doses (52.5, 105, 210, 420 μg) in 5 mM TrisHCl (pH 7.4) containing 150 mM NaCl and 175 μM $CaCl_2$, while animals were permanently ventilated. The same volume of buffer (2.5 ml/kg body weight) was instilled in the rat lungs of the control group. In the CRP/SP-A-coinstilled group, both proteins were instilled at a CRP/SP-A molar ratio of 5:1. Both proteins were dissolved in the same buffer and the instillation volume was 2.5 ml/kg. After CRP or CRP/SP-A instillation, animals were ventilated for 150 min with the assigned ventilation parameters.

At the end of the experiment, a bronchoalveolar lavage was performed. The total number of BAL cells and the cell viability were determined. Cell-free BAL was used for protein determination, CRP quantification by ELISA (Chemicon International, Temecula, CA, USA) and lung surfactant isolation, as reported by Casals *et al.* (16, 26). Isolated rat lung surfactant, which contains hydrophobic surfactant proteins (SP-B and SP-C), SP-A, surfactant phospholipids, and cholesterol, was used to analyze the biophysical activity of surfactant at a phospholipid concentration of 75 μM in all samples.

Isolation and analysis of the lipid organic extract of surfactant

Pulmonary surfactant from both rat and porcine lungs were obtained as described previously (16, 26). The organic extract of rat or porcine lung surfactant, which contains surfactant lipids, SP-B, and SP-C, was obtained by chloroform/methanol extraction (16). Total phospholipid (PL) was determined by phosphorus analysis, and phospholipid classes were analyzed by thin-layer chromatography (16). Total surfactant cholesterol was determined enzymatically using the Sigma Diagnostic Cholesterol Kit. SP-B and SP-C content was determined in organic extracts of porcine surfactant using ELISA procedures described previously (26). The protein and lipid com-

position of lipid organic extract of porcine surfactant is detailed by Saenz *et al.* (27).

Surfactant liposomes

From the lipid organic extract of surfactant, we formed different types of liposomes: multilamellar vesicles (MLVs), large unilamellar vesicles (LUVs), and giant unilamellar vesicles (GUVs) in 5 mM Tris-HCl (pH 7) containing 150 mM NaCl (buffer A). These liposomes are referred to as "lipid extract surfactant" (LES) from pig (pLES) or rat (rLES). MLVs were prepared by hydrating the dry proteolipid film, with or without fluorescent probes, in buffer A, and allowing them to swell for 1 h at 45°C. After vortexing, the resulting multilamellar vesicles were used for different assays. LUVs of 120 ± 20 nm were prepared at 45°C in buffer A with a Mini-Extruder (Avanti Polar Lipids, Birmingham, AL, USA), according to the manufacturer's instructions. For vesicle-size analysis, dynamic light scattering was used as described below. A new electroformation method was used to obtain the GUVs from the lipid organic extract of surfactant under physiological conditions (28). The lipid organic extract of surfactant was first labeled with either DiI_{C18} or LAURDAN with the percentage of fluorescent probe in the sample less than 0.1 mol %. MLVs, LUVs, or GUVs of protein-free surfactant-like vesicles composed of DPPC/POPG/PA (28:9.4:5.1, w/w/w), were also prepared. This is a well-characterized lipid mixture typically used in the formulation of new synthetic lung surfactants (27).

Interfacial adsorption assays

The effect of different CRP concentrations on the ability of either lung surfactant or lipid extract surfactant to adsorb onto and spread at an air-water interface was analyzed with a Wilhelmy-like highly sensitive surface microbalance coupled to a small Teflon dish, as previously reported (16, 22–24, 26, 27). Multilamellar vesicles of lung surfactant or LES (75 or 150 μM phospholipids) were injected into the hypophase chamber of the Teflon dish, which contained 6 ml of 150 mM NaCl, 25 mM HEPES buffer, pH 7.0 (buffer B) containing 2.5 mM $CaCl_2$. Interfacial adsorption was measured following the change in surface tension as a function of time.

Monolayer experiments

Monolayer experiments were performed at 25°C using a thermostatted Langmuir-Blodgett trough (102M micro Film Balance; NIMA Technologies, Coventry, UK) equipped with an injection port and magnetically stirred. The trough is equipped with two symmetrical movable barriers controlled by an electronic device. A concentrated solution (1 mg/ml) of the lipid organic extract of porcine lung surfactant dissolved in chloroform/methanol 3/1 (v/v) was used for monolayer experiments. The subphase employed was buffer A. For penetration studies, monolayers were formed by spreading 10 μl of a concentrated solution of the lipid organic extract of surfactant at the air-water interface to give the indicated initial surface pressures (from 7 to 30 mN/m). After organic solvent evaporation, the monolayer was allowed to stabilize for a few minutes before 100 μl of a stock solution of either CRP, SP-A, or the mixture CRP+SP-A was injected into the subphase without disturbing the lipid monolayer. Then, protein-induced changes in the monolayer surface pressure at constant surface area were measured.

Fluorescence experiments

Fluorescence experiments were carried out as described previously (22–24, 27), using an SLM-Aminco AB-2 spectrofluorimeter equipped with Glam Prism polarizers and a thermostat-regulated cuvette holder (±0.1°C; Thermo Spectronic, Waltham, MA, USA). Quartz cuvettes of 5- × 5-mm path length were used.

Fluorescence emission anisotropy

The required amounts of phospholipids from the lipid organic extract of surfactant were mixed with DPH at a probe/phospholipid molar ratio of 1:200 (final phospholipid concentration of 1 mg/ml). The same DPH/lipid ratio was used for the DPPC/POPG/PA (28:9.4:5.1, w/w/w) mixture. After LUV formation in buffer A, CRP (at different concentrations) was added in the absence and presence of physiological concentrations of SP-A (2.5% of the total mass of surfactant lipids). Fluorescence emission anisotropy measurements were obtained with Glan Prism polarizers at 37°C as previously reported (27). Excitation and emission wavelengths were set at 360 and 430 nm, respectively.

DPH fluorescence quenching by TEMPO

The lipid organic extract of surfactant, DPH, and TEMPO (when required) were mixed at a 300:1:1 molar ratio (final phospholipid concentration of 1 mg/ml). LUVs were then prepared in buffer A, and different amounts of CRP in the absence and presence of 2.5 wt % SP-A were added. Fluorescence emission of DPH was recorded at 428 nm (λ_{ex}=360 nm) at 37°C.

LAURDAN GP function

The lipid organic extract of surfactant was mixed with LAURDAN at a probe/phospholipid molar ratio of 1:100. LUVs were prepared in buffer A and then steady-state fluorescence emission spectra of LAURDAN were measured at 25°C in the absence and presence of different CRP concentrations on excitation at 364 nm. The LAURDAN emission maximum is near 440 nm in the lipid gel phase but red-shifted to 490 nm in the liquid-crystalline phase (29). To quantify these emission spectrum changes, the excitation generalized polarization (GP_{ex}) of LAURDAN was calculated according to Parasassi *et al.* (29) using Eq. 1:

$$GP = \frac{I_B - I_R}{I_B + I_R} \quad (1)$$

where I_B and I_R are the intensities at the blue (440 nm) and red (490 nm) limits of the emission spectrum (λ_{ex}=364 nm).

Observation of giant vesicles

An inverted confocal excitation fluorescence microscope (Zeiss LSM 510 META; Carl Zeiss, Jena, Germany) was used for the 1-photon excitation experiments (using the probe DiIC18). The excitation wavelength was 543 nm, and the fluorescence signal was collected using bandpass filters of 590 ± 25 nm. A custom-built 2-photon excitation fluorescence microscope was utilized to obtain the LAURDAN GP images. The excitation wavelength used was 780 nm, and the fluorescence signals were simultaneously collected in two different channels using bandpass filters of 438 ± 12 nm and 494 ± 10 nm (28). Unilamellarity was assured by measuring the fluorescence intensity of the equator region as described previously. The LAURDAN GP images were computed with

the SimFCS software (Laboratory for Fluorescence Dynamics, Irvine, CA) using fluorescence intensity images obtained simultaneously in the blue and red regions of LAURDAN emission spectra.

Differential scanning calorimetry

Calorimetric measurements were performed as previously reported (24, 27) in a Microcal VP differential scanning calorimeter (Microcal Inc., Northampton, MA, USA) at a heating rate of 0.5°C/min. Multilamellar vesicles (1 mM) of either pLES or DPPC/POPG/PA (28:9.4:5.1, w/w/w), in the absence and presence of CRP and/or SP-A, were loaded in the sample cell of the microcalorimeter with 0.6 ml of buffer B containing 0.2 mM $CaCl_2$ in the reference cell. Three calorimetric scans were collected from each sample between 15 and 65°C. The standard Microcal Origin software was used for data acquisition and analysis. The excess heat capacity functions were obtained after subtraction of the buffer-buffer base line.

Solid-phase binding assay

To explore whether SP-A binds to immobilized CRP, solid-phase binding assay was performed with biotinylated SP-A. Either CRP or human serum albumin (1 μg) was coated on the wells of a 96-well maxisorp microtiter plate (Nunc, Rochester, NY, USA) in 0.1 mM sodium bicarbonate buffer, pH 9.7, containing 0.2 mM Ca_2Cl, overnight at 4°C. The wells were washed three times with washing buffer (5 mM Tris-HCl, pH 7.4, containing 150 mM NaCl, 0.1% Tween 20). Wells were blocked with buffer containing 5% nonfatty dried milk for 2h. After the plate was washed, biotinylated SP-A in concentrations ranging 0 to 470 nM was added to the wells in the same buffer containing 2 mM $CaCl_2$ with or without 0.4 mM phosphocholine. Incubations were performed for 1 h at room temperature. After extensive washing, streptavidin-horseradish peroxidase was added to the wells. The bound biotin-labeled SP-A was detected with *o*-phenylenediamine dihydrochloride tablets. The colorimetric reaction was stopped with 4 M sulfuric acid, and the absorbance in each well was read at 490 nm on an ELISA reader (DigiScan; Asys HiTech GmbH, Eugendorf, Austria).

Dynamic light scattering

The hydrodynamic diameters of CRP and SP-A, as well as mixtures of these components were measured at 25°C in a Zetasizer Nano S (Malvern Instruments, Malvern, UK) equipped with a 633-nm HeNe laser. Six scans were performed for each sample, and all of the samples were analyzed in triplicate. The hydrodynamic diameter was calculated using the general purpose algorithm available from the Malvern software for dynamic light scattering analysis, which correlates the diffusion coefficient to the hydrodynamic diameter through the Stokes-Einstein equation, Eq. 2:

$$d_H = \frac{k_B T}{3\pi\eta D} \quad (2)$$

where k_B is the Boltzmann constant, T is the temperature, η is the viscosity, and D is the translational diffusion coefficient. The multiple narrow modes algorithm was also used to verify the results obtained by the general purpose method. The interaction of SP-A with CRP in solution was measured by the addition of different SP-A concentrations (from 0 to 150 nM) to 0.67 μM CRP in buffer A containing either 175 μM or 2.5 mM $CaCl_2$.

Statistical analyses

Means were compared by 1-way ANOVA. We considered $P < 0.05$ as statistically significant. Data are shown as means ± SE. The statistical package SPSS 15.0 (SPSS Inc., Chicago, IL, USA) was used for the analysis.

RESULTS

In vivo and in *vitro* effects of CRP and CRP+SP-A on lung surfactant

The effects of CRP and CRP+SP-A *in vivo* were evaluated by intratracheal administration of these proteins in rat lungs. Animals were maintained for a short time (150 min) under a protective ventilation strategy (V_T=9 ml/kg and PEEP=5 cmH_2O) to avoid adverse effects of either prolonged benign mechanical ventilation on lung surfactant or short-term high V_T mechanical ventilation on lung function. The amount of human CRP that reaches the alveolar fluid was determined by ELISA and expressed as percentage CRP/phospholipid weight ratio. Surfactant function was determined by measuring the ability of the whole surfactant isolated from these animals to adsorb onto and spread at an air-water interface. We found that ~15 wt % CRP in the alveolar fluid significantly inhibited surfactant surface adsorption (**Fig. 1*A***). 15 wt % CRP corresponds to ~9.9 μg CRP/ml BAL and ~282 μg CRP/kg body weight. These quantities are, in fact, comparable to those that we found under pathological conditions (175 μg BAL CRP/kg body weight; ~10 wt % CRP in the alveolar fluid) in a rat model of acute lung injury induced by high V_T mechanical ventilation (unpublished results). The inset of Fig. 1*A* shows surface pressure as a function of CRP concentration recovered in BAL expressed as percentage CRP/phospholipid weight ratio. Surfactant inhibition increased with increasing CRP concentration. We did not find alveolar edema and/or markers of inflammation (TNF-α, IL6, neutrophil infiltration) in BAL from the CRP group (data not shown). This suggests that surfactant recovered from these animals does not seem to be damaged by secondary insults different than CRP. Notably, Fig. 1*A* also shows that coinstillation of SP-A (at a CRP/SP-A molar ratio of 5:1) blocked the inhibitory effects of CRP.

Concentrations of CRP required to inhibit surface adsorption of the whole surfactant *in vivo* were greater than those needed *in vitro* to inhibit LES vesicles, which lack SP-A (data not shown). Figure 1*B* shows adsorption kinetics of LES at a phospholipid concentration similar to that used for experiments in Fig. 1*A* (75 μM phospholipid). Under these conditions, the equilibrium pressure was not attained (solid squares) unless SP-A, at physiological concentrations (2.5 wt %), was added to the medium (solid circles). The presence of 10 wt % CRP in the subphase-inhibited surface adsorption of

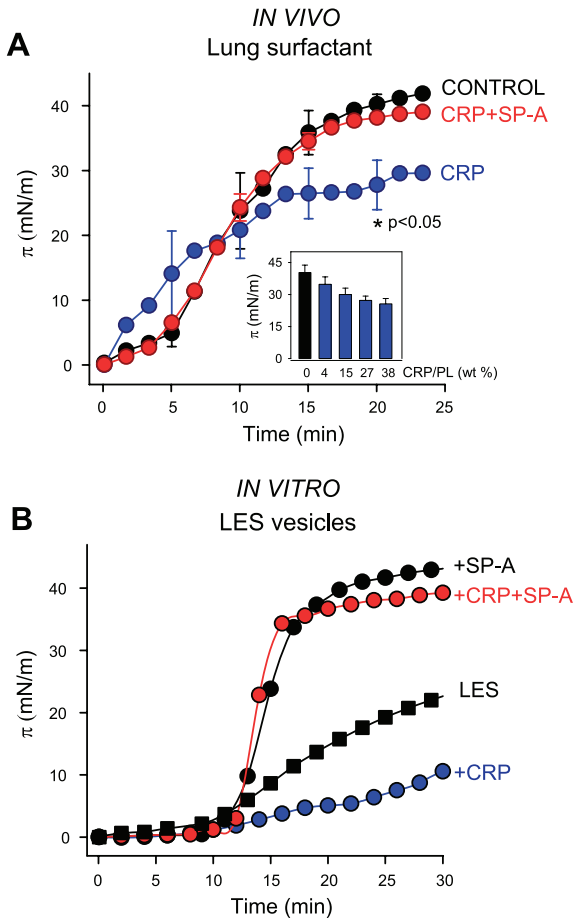

Figure 1. *A*) Intratracheal instillation of CRP in rat lungs inhibits surfactant surface adsorption, and coinstilled SP-A blocks CRP inhibitory effects. Surface adsorption analysis from lung surfactant isolated from these animals was performed at a phospholipid concentration of 75 μM. Data are expressed as means ± SD. Differences between CRP-instilled rat lungs (n=5) *vs.* control (n=5) and CRP+SP-A-coinstilled (n=5) rat lungs were significant (P<0.05). For these experiments, the CRP concentration recovered in BAL after 150 min ventilation was ~15% CRP/phospholipid weight ratio. The CRP/SP-A molar ratio was 5:1. Inset: surface pressure as a function of CRP concentration recovered in BAL. *B*) *In vitro* analysis of CRP inhibitory effect on lipid extract surfactant (LES). Surface adsorption was assayed at a phospholipid concentration of 75 μM, in the absence and presence of CRP (10 wt %) and/or SP-A (2.5 wt%). Values are means of 3 experiments.

LES, which was completely reversed by SP-A at a CRP/SP-A molar ratio of 5:1. Similar results were obtained with pLES or rLES.

Mechanisms by which CRP induces alterations in lung surfactant membranes

CRP inserts into surfactant membranes

Phospholipid monolayers at an air-water interface provide a simple model for mimicking biological membranes. Insertion of proteins into a membrane can be monitored by measuring increases in the lipid monolayer surface pressure. Thus, proteins that only interact with the lipid head groups, without insertion among the lipid molecules, do not induce an increase in surface pressure (30, 31). **Figure 2*A*** shows that injection of CRP into the aqueous subphase (18.2 ng/ml, final concentration) resulted in a rapid increase in the monolayer surface pressure, which reached a plateau (equilibrium adsorption pressure π_e) ~5 min after CRP injection.

By plotting the surface pressure increase ($\Delta\pi = \pi_e - \pi_o$) as a function of initial surface pressure (π_o), the maximum insertion pressure (MIP) is determined by extrapolation of the regression line to a surface pressure increase equal to 0 (Fig. 2*B*). This parameter corresponds to the initial surface pressure of surfactant monolayer, above which no more CRP molecules can penetrate the lipid film and increase surface pressure. In addition, the $\Delta\pi_{max}$ is obtained by extrapolating the regression of the plot to the *y* axis. Our results show that CRP inserted in surfactant monolayers with MIP = 34 mN/m and $\Delta\pi_{max}$ = 14 mN/m. In monolayers of surfactant-like lipids that do not contain surfactant proteins and cholesterol [DPPC/POPG/PA (28:9.4:5.1, w/w/w)], a reduced MIP and $\Delta\pi_{max}$ (28 and 8.5 mN/m, respectively) was obtained (Fig. 2*B*).

Lung surfactant monolayers and monolayers composed of surfactant-like lipids show liquid-expanded (LE) and tilted-condensed (TC) coexisting domains, which persist to $\pi \geq 35$ and 30 mN/m, respectively (17, 27). In contrast, pure DPPC monolayers show LE-TC phase coexistence at π = 7–12 mN/m (17). At π = 21 mN/m, pure DPPC monolayers consist of a homogeneous TC phase, and CRP molecules cannot penetrate the DPPC film (MIP=21 mN/m). In POPC monolayers, which show a single liquid-expanded state, a MIP of 24.5 mN/m has been obtained for CRP (data not shown). This suggests that CRP hardly penetrates membranes composed of either DPPC or POPC, given that the membrane lateral pressure has been estimated in the range of ~30–35 mN/m (30, 31).

When CRP is preincubated with SP-A before injection at a CRP/SP-A molar ratio of 5:1 (Fig. 2*A*, open circles), its ability to insert into the lipid monolayer significantly decreased to values similar to those obtained for SP-A alone (18.2 ng SP-A/ml subphase) (Fig. 2*C*, shaded circles). Similar results were obtained when CRP was injected 10 min after SP-A injection: the presence of SP-A blocked CRP's ability to insert into the lipid monolayer (Fig. 2*C*, open circles). Moreover, injection of SP-A 10 min after insertion of CRP into the monolayer caused a rapid decrease in the surface pressure (Fig. 2*D*). Taken together, these results demonstrate that CRP's ability to insert into the membrane disappears in the presence of SP-A.

CRP causes disappearance of liquid-ordered/ liquid-disordered phase coexistence

Given that CRP inserts into surfactant membranes, we study the effects of CRP on the lipid lateral organiza-

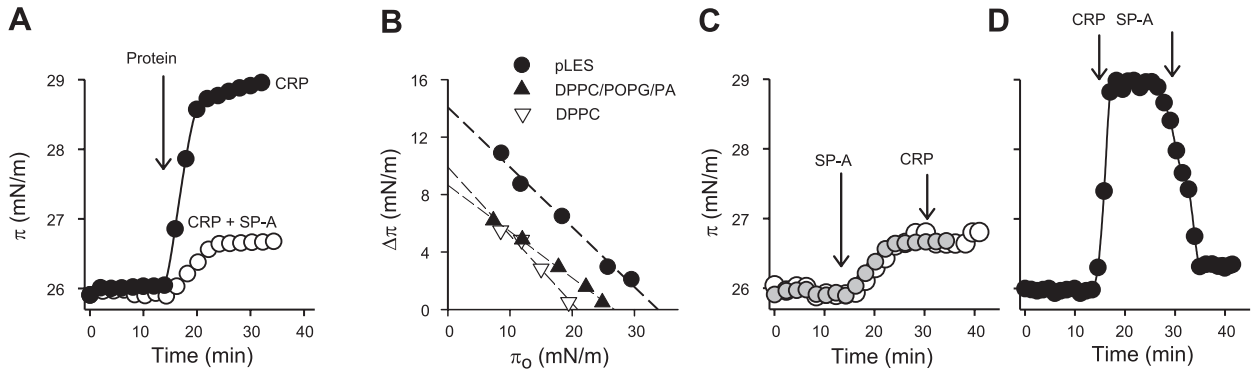

Figure 2. CRP inserts into surfactant monolayers, and SP-A abrogates CRP insertion. *A*) Surface pressure profile of pLES monolayers after injecting CRP alone (solid circles) and CRP plus SP-A (open circles) in the subphase. *B*) Surface pressure increase is induced by the insertion of CRP into pLES, DPPC/POPG/PA, or DPPC monolayers as a function of the initial surface pressure. Straight line was obtained by linear regression. *C*, *D*) Surface pressure profile of pLES monolayers after injecting the following proteins in the subphase: SP-A alone (shaded circles), and sequential injection of SP-A and 10 min after CRP in the subphase (open circles) (*C*); and sequential injection of CRP and 10 min after SP-A in the subphase (*D*). Arrows indicate time when proteins were injected into the stirred subphase. Final concentration of either CRP or SP-A in the subphase was 18.2 ng/ml. One representative experiment of 3 is shown. $T = 25.0 \pm 0.1$°C.

tion of pLES membranes by confocal fluorescence microscopy of GUVs. Vesicles of pLES doped with the fluorescent probe DiI_{c18} were imaged in the top region (**Fig. 3**). GUVs of pLES exhibited the typical liquid-ordered/liquid-disordered (L_o/L_d) phase coexistence previously reported (27, 32), which is characterized by the presence of fluorescent round domains over a dark background. GUVs composed of surfactant-like lipids (DPPC/POPG/PA, 28:9.4:5.1, w/w/w), which contain no surfactant proteins and cholesterol, show solid/fluid (L_β/L_α) phase coexistence (27). The fluorescent dye is present in the fluid domains and is excluded from the micrometer-sized solid domains, which appear black. The addition of CRP to GUVs composed of pLES or surfactant-like lipids caused disappearance of the l_o/l_d phase coexistence (pLES) or L_β/L_α phase coexistence (DPPC/POPG/PA) typical of these membranes. This would signify that, in the presence of CRP, micrometer-sized ordered domains disappear. Figure 3 also shows that preincubation of CRP and SP-A before the addition to GUVs blocked CRP effects and preserved micrometer-sized ordered/disordered phase coexistence of these vesicles. SP-A alone had no effect on the phase coexistence of surfactant membranes (27).

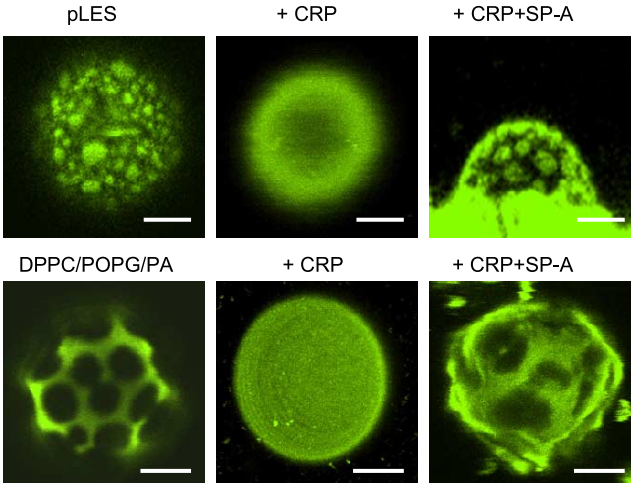

Figure 3. CRP causes disappearance of ordered/disordered-phase coexistence of surfactant membranes. CRP effects on the lipid lateral organization of GUVs (0.2 mg/ml) prepared from either pLES or DPPC/POPG/PA (28:9.4:5.1, w/w/w) were studied in the absence and presence of SP-A. GUVs were doped with the fluorescent probe DiI_{C18}. Images were taken at 25°C. Final concentrations of CRP and SP-A were 20 and 5 μg/ml, respectively. SP-A alone had no effect on the lipid lateral organization of these vesicles. Scale bars = 5 μm.

CRP increases membrane fluidity

Several approaches were used to assess that CRP influenced membrane fluidity in pLES.

DPH anisotropy **Figure 4*A*** shows that addition of increasing concentrations of CRP to pLES unilamellar vesicles at 37°C resulted in a significant decrease in the steady-state emission anisotropy of DPH incorporated in these vesicles. To find out whether the decrease in DPH anisotropy was due to a fluidizing effect of CRP rather than caused by other factors that influence the fluorescence intensity of DPH, we determined the effect of different amounts of CRP on the fluorescence emission spectra of DPH in pLES vesicles on excitation at 340 nm (Fig. 4*B*, solid triangles). The lack of changes in the fluorescence emission of DPH with increasing amounts of CRP suggests that CRP decreases the lipid order of pLES membranes. Remarkably, in the presence of 2.5 wt% SP-A, the CRP-induced decrease in DPH anisotropy was reversed (Fig. 4*A*). Since SP-A alone does not influence the lipid order of pLES membranes (27), these results suggest that SP-A counteracts CRP-fluidizing effects by inhibiting CRP ability to insert into the membrane (Fig. 2).

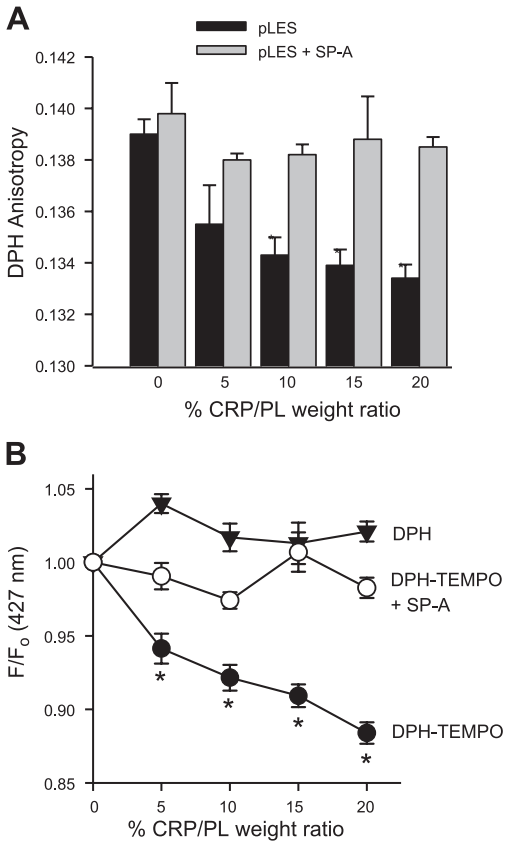

Figure 4. CRP increases membrane fluidity. *A*) Effect of increasing CRP concentrations on steady-state anisotropy of DPH embedded in pLES unilamellar vesicles (1 mg/ml). Experiments were performed in the absence and presence of 2.5 wt % SP-A at 37°C (λ_x=360 nm, λ_m=430 nm). Values are expressed as means ± SD of 3 experiments. *B*) Effect of increasing CRP concentrations on TEMPO-quenching of DPH fluorescence emission. pLES unilamellar vesicles (1 mg/ml) containing DPH with and without TEMPO, were incubated with increasing CRP concentrations. Experiments were performed in the absence and presence of 2.5 wt % of SP-A at 37°C. *F* and F_o are corrected emission intensities at 427 nm in the presence and absence of CRP, respectively. Values are means ± SD of 3 experiments. *$P < 0.05$ *vs.* pLES and pLES+ SP-A

TEMPO-quenching of DPH fluorescence The fluidizing effect of CRP was further explored by analyzing the quenching of DPH fluorescence by the stable radical TEMPO. DPH is known to distribute uniformly over either L_o or L_d domains, while TEMPO only partitions into L_d domains. Given that pLES membranes exhibit coexistence of two distinct micrometer-sized fluid phases (L_o and L_d phases) at 22–38°C, as determined by fluorescence and atomic force microscopy (27, 32), TEMPO would able to quench the fluorescence emission of DPH that partitions into L_d but not L_o domains. Figure 4*B* shows that the addition of increasing CRP concentrations to pLES unilamellar vesicles caused a decrease of DPH fluorescence emission intensity in pLES vesicles containing TEMPO, but not in those pLES vesicles without TEMPO. These results indicate that CRP has a fluidizing effect on surfactant membranes, which increases the susceptibility of DPH to quenching by TEMPO. As expected, in the presence of physiological concentrations of SP-A, the fluorescence emission of DPH in the presence of TEMPO did not change with increasing CRP concentration. Thus, the CRP fluidizing effect was reversed by SP-A.

LAURDAN fluorescence To examine whether CRP affects membrane properties near the bilayer surface, we employed the amphiphilic fluorescent dye LAURDAN, which is localized near the polar headgroups and its fluorescence emission intensity and maximum emission wavelength are influenced by the number and/or mobility of water molecules present at the membrane interface (28, 29). **Figure 5*A*** shows the emission spectrum of LAURDAN incorporated in LUVs of pLES, at 25°C, in the absence and presence of CRP. In the absence of CRP, the LAURDAN spectrum shows a maximum centered at 440 nm, denoting that these membranes contain a high percentage of ordered phase at room temperature. The addition of increasing CRP concentrations caused a progressive decrease in the fluorescence emission intensity at 440 nm and the appearance of a shoulder at ~490 nm, which indicates that the probe is in a more fluid environment. Figure 5*B* shows that the LAURDAN GP value decreased with increasing CRP concentrations, indicating that CRP is fluidizing pLES membranes.

To further assess CRP fluidizing effects on pLES membranes, we performed 2-photon fluorescence microscopy of GUVs of pLES labeled with LAURDAN. Figure 5*C, D* shows the LAURDAN GP images and the respective GP histograms of GUVs in the absence and presence of CRP or CRP+SP-A. These images represent an *x-y* plane passing through the center of the GUV. At 25°C, the LAURDAN GP histogram of pLES was centered at GP values of ~0.42 (Fig. 5*D*). This is consistent with fluorescence experiments with LUVs shown in Fig. 5*B*. After CRP addition, the LAURDAN GP value decreased to ~0.14. Preincubation of CRP and SP-A before addition to GUVs resulted in an increase of LAURDAN GP values with respect to those obtained with CRP alone. SP-A alone had no effect on 2-photon excitation LAURDAN GP images of pLES (data not shown) (32).

The fluidizing effects of CRP have also been demonstrated in LUVs and GUVs composed of surfactant-like lipids DPPC/POPG/PA (28:9.4:5.1, w/w/w), and CRP fluidizing effects were also reduced in the presence of SP-A (data not shown).

CRP decreases the phase transition enthalpy of lung surfactant membranes

We have used differential scanning calorimetry to probe the effect of CRP and/or SP-A on the thermotropic properties of pLES and DPPC/POPG/PA multilamellar vesicles (**Fig. 6** and **Table 1**). Compared to DPPC/POPG/PA, the thermal transition of pLES membranes exhibited a broader melting event with

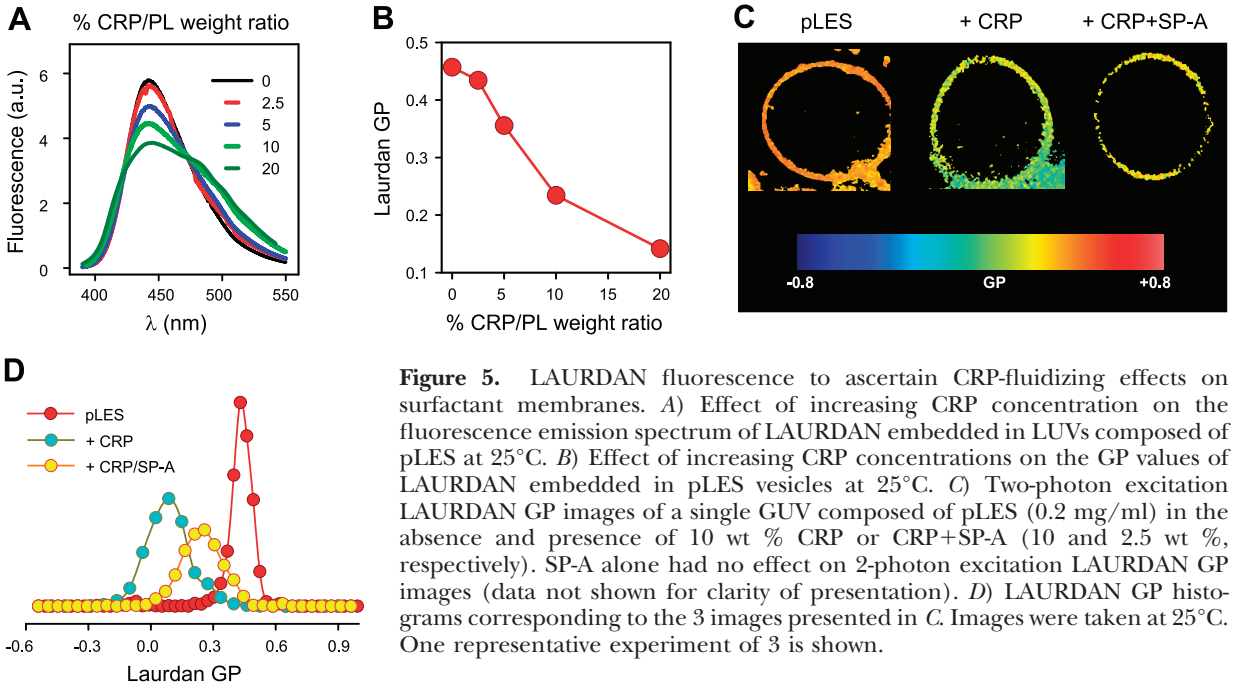

Figure 5. LAURDAN fluorescence to ascertain CRP-fluidizing effects on surfactant membranes. *A*) Effect of increasing CRP concentration on the fluorescence emission spectrum of LAURDAN embedded in LUVs composed of pLES at 25°C. *B*) Effect of increasing CRP concentrations on the GP values of LAURDAN embedded in pLES vesicles at 25°C. *C*) Two-photon excitation LAURDAN GP images of a single GUV composed of pLES (0.2 mg/ml) in the absence and presence of 10 wt % CRP or CRP+SP-A (10 and 2.5 wt %, respectively). SP-A alone had no effect on 2-photon excitation LAURDAN GP images (data not shown for clarity of presentation). *D*) LAURDAN GP histograms corresponding to the 3 images presented in *C*. Images were taken at 25°C. One representative experiment of 3 is shown.

lower melting enthalpy (ΔH) due to the complex lipid composition of these membranes and the presence of cholesterol. The addition of 10 wt % CRP to multilamellar vesicles of pLES or DPPC/POPG/PA caused a decrease in the melting enthalpy without modifying the gel to fluid main transition temperature (T_m) of these vesicles. These CRP effects might be explained by a decrease of van der Waals interactions between lipid acyl chains after protein insertion, as has been reported for other proteins (33). Figure 6 and Table 1 also show that SP-A counteracted CRP effects on the melting enthalpy of surfactant membranes. Since SP-A alone did not influence the thermotropic behavior of pLES (Table 1), these results suggest that SP-A counteracts CRP effects on the melting enthalpy by inhibiting CRP ability to insert into these membranes.

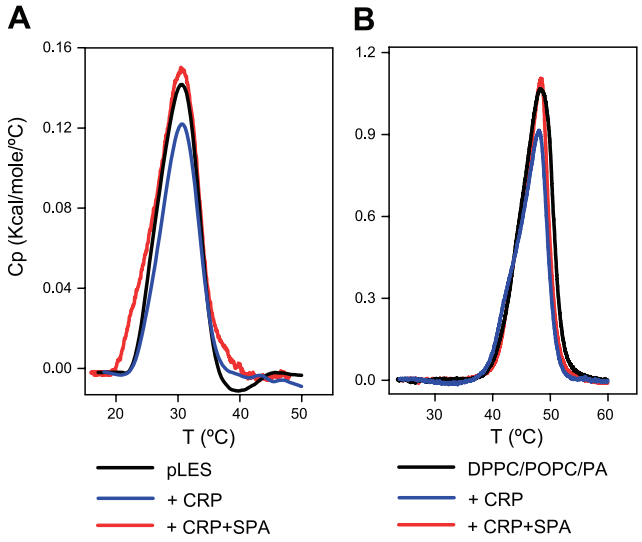

Figure 6. CRP decreases the phase transition enthalpy of either pLES or DPPC/POPG/PA multilamellar vesicles. Effect of CRP on DSC heating scans of pLES (*A*) and DPPC/POPG/PA (28:9.4:5.1, w/w/w) (*B*) multilamellar vesicles was studied in the absence (black line) and presence of 10 wt % CRP (blue line) or CRP + SP-A (10 and 2.5 wt %, respectively) (red line). SP-A alone had no effect on the thermotropic behavior of these vesicles (Table 1). Calorimetric scans were performed at a rate of 0.5°C/min. Three consecutive scans were recorded for each sample. One representative experiment of 3 is shown.

SP-A binds to CRP

Next, we determined the mechanism by which SP-A abrogates CRP insertion and blocks CRP fluidizing effects on surfactant membranes. First, we studied the potential interaction between SP-A and CRP by solid-phase binding assay. **Figure 7*A*** shows that biotinylated SP-A bound to CRP-coated wells in a dose-dependent manner, with K_d = 56 ± 8 nM. SP-A did not bind to

TABLE 1. *Thermodynamic data of MLV (1 mM) composed of pLES or DPPC/POPG/PA (28:9.4:5.1, w/w/w) in the absence and presence of CRP, SP-A, and CRP/SP-A (10 and 2.5 wt %, respectively)*

Sample	T_m (°C)	$T_{1/2}$ (°C)	ΔH (kcal/mol)
pLES	30.6 ± 0.1	8.4 ± 0.4	2.2 ± 0.1
+ SP-A (2.5 wt %)	30.8 ± 0.1	8.8 ± 0.4	2.4 ± 0.1
+ CRP (10 wt %)	30.8 ± 0.1	7.8 ± 0.4	1.4 ± 0.2*
+ CRP + SP-A	30.7 ± 0.1	8.7 ± 0.3	2.2 ± 0.1
DPPC/POPG/PA	48.5 ± 0.1	7.7 ± 0.4	12.3 ± 0.2
+ SP-A (2.5 wt %)	49.1 ± 0.1	6.2 ± 0.3	11.1 ± 0.2
+ CRP (10 wt %)	48.4 ± 0.1	6.8 ± 0.4	8.4 ± 0.2*
+ CRP + SP-A	48.4 ± 0.1	6.5 ± 0.4	12.0 ± 0.2

Data are means ± SD of 3 experiments. *$P < 0.5$.

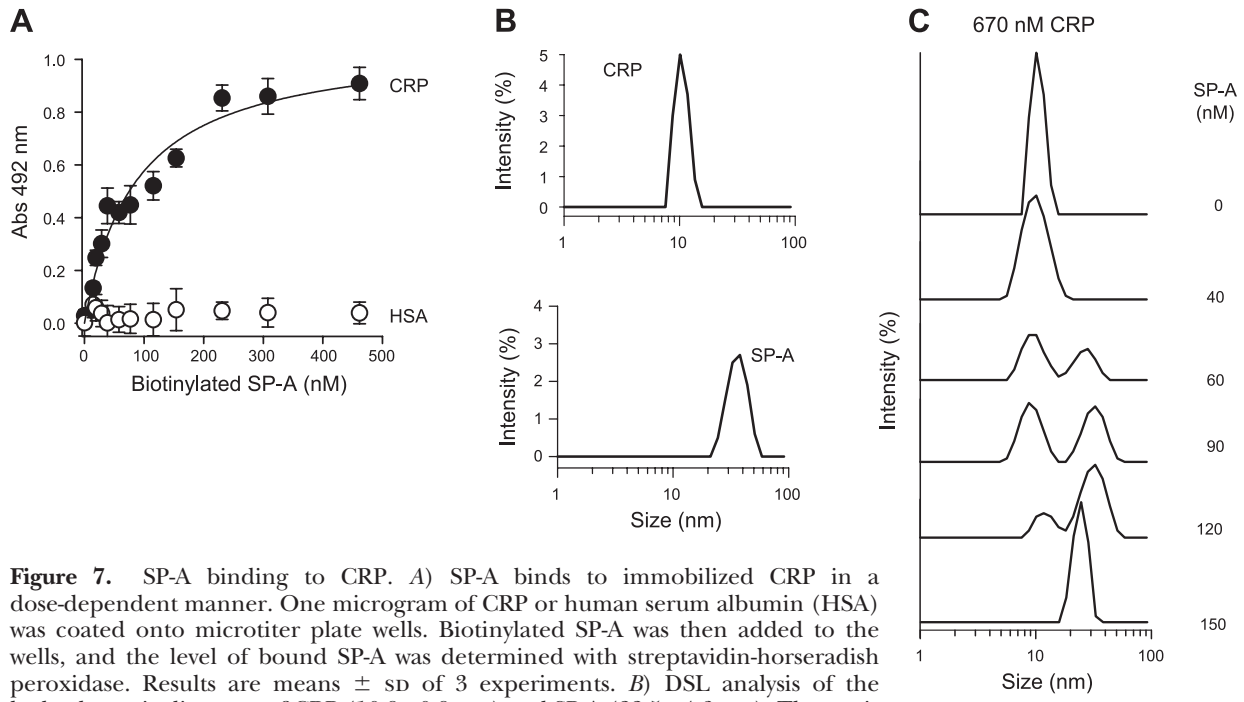

Figure 7. SP-A binding to CRP. *A*) SP-A binds to immobilized CRP in a dose-dependent manner. One microgram of CRP or human serum albumin (HSA) was coated onto microtiter plate wells. Biotinylated SP-A was then added to the wells, and the level of bound SP-A was determined with streptavidin-horseradish peroxidase. Results are means ± SD of 3 experiments. *B*) DSL analysis of the hydrodynamic diameter of CRP (10.9±0.9 nm) and SP-A (33.5±4.6 nm). The *y* axis represents the relative intensity of the scattered light; the *x* axis denotes the hydrodynamic diameter of the particles present in the solution. *C*) Addition of increasing concentrations of SP-A to a solution containing a constant concentration of CRP (0.67 μM). One representative experiment of 3 is shown.

wells coated with human serum albumin (Fig. 7*A*, open circles) or wells containing buffer alone. In addition, the binding of biotinylated SP-A to immobilized CRP was not inhibited by the presence of phosphocholine in the medium, which is the principal CRP ligand (data not shown).

The interaction of SP-A with CRP in solution was examined by dynamic light scattering. CRP alone shows a unique peak, which corresponds to particles with a hydrodynamic diameter of 11 ± 0.9 nm (Fig. 7*B*). This particle size is in accordance with the diameter of the pentamer determined by X-ray crystallography (1). In contrast, two identifiable peaks were recognized for SP-A alone, one corresponding to SP-A particles with a hydrodynamic diameter of 34 ± 5 nm (Fig. 7*B*) and another corresponding to SP-A aggregates with a hydrodynamic diameter of ~1000 nm (data not shown). Self-aggregation of SP-A occurs in the presence of calcium and NaCl (34). To reduce SP-A self-aggregation, experiments were performed in the presence of 175 μM $CaCl_2$.

Figure 7*C* shows that the addition of increasing concentrations of SP-A (ranging from 0 to 0.15 μM) to a CRP solution (0.67 μM) caused an SP-A concentration-dependent decrease of the CRP peak. At CRP/SP-A molar ratio of ~5:1, only one peak is observed with a hydrodynamic diameter of 24 ± 3 nm. This new peak, which presumably consists of SP-A+CRP, exhibited a hydrodynamic diameter lower than that observed for SP-A alone (34±5 nm), suggesting structural changes in SP-A as a consequence of the formation of the complex SP-A+CRP. The disappearance of the characteristic CRP peak of 11 nm and the appearance of the CRP/SP-A peak (24±3 nm) also occurred in the presence of excess phosphocholine, indicating that the binding of phosphocholine to CRP does not affect the interaction between CRP and SP-A.

DISCUSSION

C-reactive protein is one of the most characteristic acute-phase proteins displaying rapid and pronounced increase of concentration in serum in response to inflammation or infection (1–4). Increases in CRP were also detectable in the bronchoalveolar fluid of individuals with lung injury (11, 12, 16). BAL CRP could issue from alveolar epithelial cells (13, 14) and/or macrophages (15) stimulated by inflammatory mediators, or from the blood as a result of increased alveolar-capillary permeability. Increases in BAL CRP might inhibit lung surfactant function since several *in vitro* studies demonstrated that CRP is a potent inhibitor of surfactant biophysical activity (11, 16, 19–21). The present study shows for the first time that intratracheal instillation of CRP in rat lungs causes surfactant inactivation (Fig. 1) and that the mechanism by which CRP alters surfactant function seems to be different from that described for other serum proteins such as albumin or fibrinogen. These serum proteins are surface active and compete with surfactant membranes for the air-water interface by spontaneous adsorption (17). In contrast, CRP is not surface active but binds to surfactant membranes (16). We found that CRP inserts into these membranes rather than binding to the

membrane surface and affects membrane physical properties.

Membranes composed of the lipid extract surfactant consist of almost equimolar amounts of saturated and unsaturated phospholipid species (85 mol%), cholesterol (15 mol%), and positively charged integral membrane proteins (SP-B and SP-C) (0.2–0.35 mol%) (27). The particular composition of these membranes results in the coexistence of specialized L_o/L_d micrometer-sized membrane domains, which are required for surfactant function (17, 27, 32). The MIP value obtained for the interaction of pentameric CRP with surfactant membranes (34 mN/m) (Fig. 2*B*) is comparable to that obtained for the interaction of monomeric CRP with lipid raft-like membranes (33 mN/m) (35), and pentameric CRP was reported to undergo partial structural rearrangements on binding to biological membranes that might lead to the formation of monomeric CRP (36). These MIP values are in the range of the estimated equilibrium lateral pressure (30–35 mN/m) for biomembranes (31). The presence of cholesterol and positive charges in the membrane surface seem to enhance the binding and insertion of CRP into lung surfactant membranes, since CRP insertion into surfactant-like monolayers composed of DPPC/POPG/PA (28:9.4:5.1, w/w/w) is reduced (Fig. 2*B*). This is consistent with the fact that cholesterol and polycations are also ligands for CRP (1, 2). The lower values of MIP for CRP in the presence of DPPC (MIP=21 mN/m) or POPC (MIP=24.5 mN/m) monolayers, compared to the estimated membrane lateral pressure of 30–35 mN/m (30, 31), suggest that CRP does not extensively penetrate DPPC (solid) or POPC (fluid) biomembranes.

A common denominator of surfactant membranes, surfactant-like membranes composed of DPPC/POPG/PA, and lipid raft-like membranes is exhibition of lateral phase separation. The presence of packing defects produced by coexisting ordered/disordered domains within these membranes would facilitate the binding and partial insertion of CRP. In the regions of phase coexistence, internal lateral pressure is effectively reduced to almost zero (31), which favors membrane binding and insertion of proteins in cell membranes (31) or in bacterial lipopolysaccharide membranes (24).

Insertion of CRP into surfactant membranes or surfactant-like membranes composed of DPPC/POPG/PA strikingly affected membrane structure and membrane lipid lateral organization (Figs. 3–6). Confocal fluorescence microscopy of single GUVs doped with DiI_{C18} showed that CRP caused disappearance of micrometer-sized L_o/L_d phase coexistence in surfactant membranes (Fig. 3). In the presence of CRP, DiI_{C18} fluorescence was uniform over the GUV surface, indicating either that there is a single phase or that ordered domains have much smaller dimensions than the optical resolution of the microscope. Consistent with this morphological information, physical measurements demonstrated that CRP drastically affects membrane fluidity: *1*) CRP binding to surfactant membranes decreased the molecular order of the lipids surrounding DPH, as determined by DPH fluorescence anisotropy (Fig. 4*A*); *2*) CRP increased the susceptibility of DPH fluorescence to quenching by TEMPO (Fig. 4*B*), a stable nitroxyl free radical that partitions only into L_d domains, indicating that CRP increased the ratio of disordered/ordered domains in surfactant membranes, consistent with confocal fluorescence microscopy analysis of GUVs; *3*) LAURDAN GP experiments in cuvette (using LUVs) and LAURDAN GP images of single GUVs using 2-photon excitation fluorescence microscopy indicate that CRP decreased phospholipid packing (Fig. 5); and *4*) insertion of CRP into surfactant membranes decreased van der Waals interactions between phospholipid acyl chains, as determined by differential scanning calorimetry (Fig. 6). Taken together, these results demonstrate the fluidizing effect of CRP on membranes and its ability to cause the disappearance of micrometer-sized ordered domains.

CRP effects on membrane fluidity correlate with CRP-induced inhibition of surfactant surface adsorption. This process involves the transport of surfactant membranes through the liquid to the air-liquid interface and the rapid insertion of phospholipids into the expanding monolayer. This bilayer-to-monolayer phase transition requires ordered/disordered phase coexistence since it seems to initiate at ordered/disordered domain boundaries (17). The fact that CRP leads to a striking disappearance of micrometer-sized DPPC-rich ordered domains and to a marked inhibition of surfactant surface adsorption activity argues that micrometer-sized ordered/disordered phase coexistence is important for surfactant function.

Another focus of this study was to investigate the mechanism by which SP-A overcomes CRP-induced surfactant inhibition *in vivo* (Fig. 1*A*). SP-A is a versatile recognition protein that binds to a great variety of immune and nonimmune ligands in the alveolar fluid and is principally involved in lung defense (18). This protein is mainly associated with surfactant lipids. However, unlike CRP, SP-A interacts with surfactant membranes peripherally, without affecting surfactant membrane fluidity and perturbing the L_o/L_d phase coexistence distinctive of these membranes (27). SP-A significantly increases aggregation of lung surfactant membranes and promotes rapid formation of surface films (Fig. 1*B*) (17, 27).

We show here for the first time that SP-A binds to CRP (K_d=56±8 nM), as determined by solid-phase binding assays and dynamic light scattering (Fig. 7). The binding of SP-A to CRP hampered CRP insertion into surfactant membranes (Fig. 2*A*). SP-A also bound to the part of CRP that extrudes from the membrane, since injection of SP-A 10 min after insertion of CRP into the monolayer caused CRP to be rapidly kicked out of the membrane (Fig. 2*D*). This protein-protein interaction between SP-A and CRP abrogates the striking effect of CRP on the lipid lateral organization of surfactant membranes (Fig. 3), and blocks CRP effects on membrane fluidity (Figs. 4 and 5) and on the

melting enthalpy of surfactant vesicles (Fig. 6). The importance of SP-A/CRP interaction in controlling damaging CRP effects on lung surfactant is confirmed *in vivo* by intratracheal coinstillation of SP-A and CRP in rats. SP-A/CRP interaction blocks the inhibitory effects of CRP on isolated lung surfactant (Fig. 1).

SP-A/CRP interactions might play an important physiological role in the lung. In the alveolar fluid of normal lungs, the amount of SP-A is much greater than that of CRP, which can be produced by stimulated alveolar macrophages and epithelial cells (13–15). Under these conditions, SP-A would counteract the adverse biological effects of CRP on lung surfactant and likely strengthen the immunomodulatory effect of CRP on human alveolar macrophages (37). However, simultaneous increases in CRP and decreases in SP-A in the alveolar space are conditions associated with lung dysfunction such as ischemia-reperfusion injury after lung transplantation (12, 16) and acute lung injury (11, 18, 38). Thus, in the face of acute inflammation, excess CRP may be deleterious since SP-A could not counteract the fluidizing effects of CRP on lung surfactant at high CRP/SP-A ratios. These studies strengthen the hypothesis that addition of recombinant SP-A to replacement surfactants for acute lung injury treatment would improve surfactant resistance to inactivation.

In summary, the present report demonstrates that CRP inserts into surfactant membranes and increases membrane fluidity. CRP also causes disappearance of L_o/L_d phase coexistence distinctive of surfactant membranes, which is characterized by micrometer-sized ordered domains. These alterations in membrane fluidity and lipid lateral organization correlate with CRP-induced lung surfactant inactivation as demonstrated by *in vitro* and *in vivo* studies. In addition, this study shows that SP-A protects pulmonary surfactant against CRP inhibition by binding to CRP. This protein-protein interaction between SP-A and CRP blocks all CRP effects on surfactant membranes, as well as CRP inhibitory effects on surface adsorption. SP-A/CRP interactions seem to be an important factor *in vivo* to control injurious effects of CRP on lung surfactant. FJ

This work was supported by Ministerio de Educación y Ciencia (SAF2006-04434 and SAF2009-07810), Instituto de Salud Carlos III (CIBERES), Comunidad de Madrid (S-BIO-0260-2006), and Fundación Médica MM. Experiments in the laboratory of L.A.B. were supported by Forskningsrådet for Natur og Univers (FNU; Denmark) and the Danish National Research Foundation.

REFERENCES

1. Volanakis, J. E. (2001) Human C-reactive protein: expression, structure, and function. *Mol. Immunol.* **38,** 189–197
2. Black, S., Kushner, I., and Samols, D. (2004) C-reactive protein. *J. Biol. Chem.* **279,** 48487–48490
3. Marnell, L., Mold, C., and Du Clos, T. W. (2005) C-reactive protein: ligands, receptors and role in inflammation. *Clin. Immunol.* **117,** 104–111
4. Casas, J. P., Shah, T., Hingorani, A. D., Danesh, J., and Pepys, M. B. (2008) C-reactive protein and coronary heart disease: a critical review. *J. Intern. Med.* **264,** 295–314
5. Christopeit, T., Gossas, T., and Danielson, U. H. (2009) Characterization of Ca^{2+} and phosphocholine interactions with C-reactive protein using a surface plasmon resonance biosensor. *Anal. Biochem.* **391,** 39–44
6. Lu, J., Marnell, L. L., Marjon, K. D., Mold, C., Du Clos, T. W., and Sun, P. D. (2008) Structural recognition and functional activation of FcγR by innate pentraxins. *Nature* **456,** 989–992
7. Singh, S. K., Suresh, M. V., Voleti, B., and Agrawal, A. (2008) The connection between C-reactive protein and atherosclerosis. *Ann. Med.* **40,** 110–120
8. Rasmussen, F., Mikkelsen, D., Hancox, R. J., Lambrechtsen, J., Nybo, M., Hansen, H. S., and Siersted, H. C. (2009) High-sensitive C-reactive protein is associated with reduced lung function in young adults. *Eur. Respir. J.* **33,** 382–388
9. Dahl, M., Vestbo, J., Lange, P., Bojesen, S. E., Tybjaerg-Hansen, A., and Nordestgaard, B. G. (2007) C-reactive protein as a predictor of prognosis in chronic obstructive pulmonary disease. *Am. J. Respir. Crit. Care Med.* **175,** 250–255
10. Levy, H., Kalish, L. A., Huntington, I., Weller, N., Gerard, C., Silverman, E. K., Celedon, J. C., Pier, G. B., and Weiss, S. T. (2007) Inflammatory markers of lung disease in adult patients with cystic fibrosis. *Pediatr. Pulmonol.* **42,** 256–262
11. Li, J. J., Sanders, R. L., McAdam, K. P., Hales, C. A., Thompson, B. T., Gelfand, J. A., and Burke, J. F. (1989) Impact of C-reactive protein (CRP) on surfactant function. *J. Trauma* **29,** 1690–1697
12. Vos, R., Vanaudenaerde, B. M., De Vleeschauwer, S. I., Willems-Widyastuti, A., Scheers, H., Van Raemdonck, D. E., Dupont, L. J., and Verleden, G. M. (2009a) Circulating and intrapulmonary C-reactive protein: a predictor of bronchiolitis obliterans syndrome and pulmonary allograft outcome. *J. Heart Lung Transplant.* **28,** 799–807
13. Gould, J. M., and Weiser, J. N. (2001) Expression of C-reactive protein in the human respiratory tract. *Infect. Immun.* **69,** 1747–1754
14. Ramage, L., Proudfoot, L., and Guy, K. (2004) Expression of C-reactive protein in human lung epithelial cells and upregulation by cytokines and carbon particles. *Inhal. Toxicol.* **16,** 607–613
15. Dong, Q., and Wright, J. R. (1996) Expression of C-reactive protein by alveolar macrophages. *J. Immunol.* **156,** 4815–4820
16. Casals, C., Varela, A., Ruano, M. L., Valino, F., Perez-Gil, J., Torre, N., Jorge, E., Tendillo, F., and Castillo-Olivares, J. L. (1998) Increase of C-reactive protein and decrease of surfactant protein A in surfactant after lung transplantation. *Am. J. Respir. Crit. Care Med.* **157,** 43–49
17. Zuo, Y. Y., Veldhuizen, R. A., Neumann, A. W., Petersen, N. O., and Possmayer, F. (2008) Current perspectives in pulmonary surfactant-inhibition, enhancement and evaluation. *Biochim. Biophys. Acta* **1778,** 1947–1977
18. Wright, J. R. (2005) Immunoregulatory functions of surfactant proteins. *Nat. Rev. Immunol.* **5,** 58–68
19. Amirkhanian, J. D., and Taeusch, H. W. (1993) Reversible and irreversible inactivation of preformed pulmonary surfactant surface films by changes in subphase constituents. *Biochim. Biophys. Acta* **1165,** 321–326
20. McEachren, T. M., and Keough, K. M. (1995) Phosphocholine reverses inhibition of pulmonary surfactant adsorption caused by C-reactive protein. *Am. J. Physiol.* **269,** L492–L497
21. Nag, K., Rodriguez-Capote, K., Panda, A. K., Frederick, L., Hearn, S. A., Petersen, N. O., Schurch, S., and Possmayer, F. (2004) Disparate effects of two phosphatidylcholine binding proteins, C-reactive protein and surfactant protein A, on pulmonary surfactant structure and function. *Am. J. Physiol. Lung Cell. Mol. Physiol.* **287,** L1145–L1153
22. Sanchez-Barbero, F., Strassner, J., Garcia-Canero, R., Steinhilber, W., and Casals, C. (2005) Role of the degree of oligomerization in the structure and function of human surfactant protein A. *J. Biol. Chem.* **280,** 7659–7670
23. Sanchez-Barbero, F., Rivas, G., Steinhilber, W., and Casals, C. (2007) Structural and functional differences among human surfactant proteins SP-A1, SP-A2 and co-expressed SP-A1/SP-A2: role of supratrimeric oligomerization. *Biochem. J.* **406,** 479–489

24. Canadas, O., Garcia-Verdugo, I., Keough, K. M., and Casals, C. (2008) SP-A permeabilizes lipopolysaccharide membranes by forming protein aggregates that extract lipids from the membrane. *Biophys. J.* **95,** 3287–3294
25. Institute for Animal Laboratory Research (1996) *Guide for the Care and Use of Laboratory Animals*, National Academy Press, Washington D.C.
26. Valino, F., Casals, C., Guerrero, R., Alvarez, L., Santos, M., Saenz, A., Varela, A., Claro, M. A., Tendillo, F., and Castillo-Olivares, J. L. (2004) Inhaled nitric oxide affects endogenous surfactant in experimental lung transplantation. *Transplantation* **77,** 812–818
27. Saenz, A., Canadas, O., Bagatolli, L. A., Sanchez-Barbero, F., Johnson, M. E., and Casals, C. (2007) Effect of surfactant protein A on the physical properties and surface activity of KL4-surfactant. *Biophys. J.* **92,** 482–492
28. Bagatolli, L. A. (2006) To see or not to see: lateral organization of biological membranes and fluorescence microscopy. *Biochim. Biophys. Acta* **1758,** 1541–1556
29. Parasassi, T., De Stasio, G., Ravagnan, G., Rusch, R. M., and Gratton, E. (1991) Quantitation of lipid phases in phospholipid vesicles by the generalized polarization of Laurdan fluorescence. *Biophys. J.* **60,** 179–189
30. Calvez, P., Bussieres, S., Eric, D., and Salesse, C. (2009) Parameters modulating the maximum insertion pressure of proteins and peptides in lipid monolayers. *Biochimie (Paris)* **91,** 718–733
31. Marsh, D. (1996) Lateral pressure in membranes. *Biochim. Biophys. Acta* **1286,** 183–223
32. Bernardino de la Serna, J., Perez-Gil, J., Simonsen, A. C., and Bagatolli, L. A. (2004) Cholesterol rules: direct observation of the coexistence of two fluid phases in native pulmonary surfactant membranes at physiological temperatures. *J. Biol. Chem.* **279,** 40715–40722
33. McElhaney, R. N. (1986) Differential scanning calorimetric studies of lipid-protein interactions in model membrane systems. *Biochim. Biophys. Acta* **864,** 361–421
34. Ruano, M. L., Garcia-Verdugo, I., Miguel, E., Perez-Gil, J., and Casals, C. (2000) Self-aggregation of surfactant protein A. *Biochemistry* **39,** 6529–6537
35. Ji, S. R., Ma, L., Bai, C. J., Shi, J. M., Li, H. Y., Potempa, L. A., Filep, J. G., Zhao, J., and Wu, Y. (2009) Monomeric C-reactive protein activates endothelial cells via interaction with lipid raft microdomains. *FASEB J.* **23,** 1806–1816
36. Ji, S. R., Wu, Y., Zhu, L., Potempa, L. A., Sheng, F. L., Lu, W., and Zhao, J. (2007) Cell membranes and liposomes dissociate C-reactive protein (CRP) to form a new, biologically active structural intermediate: mCRP(m). *FASEB J.* **21,** 284–294
37. Casals, C., Arias-Diaz, J., Valino, F., Saenz, A., Garcia, C., Balibrea, J. L., and Vara, E. (2003) Surfactant strengthens the inhibitory effect of C-reactive protein on human lung macrophage cytokine release. *Am. J. Physiol. Lung Cell. Mol. Physiol.* **284,** L466–L472
38. Gunther, A., Ruppert, C., Schmidt, R., Markart, P., Grimminger, F., Walmrath, D., and Seeger, W. (2001) Surfactant alteration and replacement in acute respiratory distress syndrome. *Respir. Res.* **2,** 353–364

Received for publication December 29, 2009.
Accepted for publication May 6, 2010.